J Biol Inorg Chem
DOI 10.1007/s00775-010-0638-x

ORIGINAL PAPER

The chemical forms of mercury in human hair: a study using X-ray absorption spectroscopy

Graham N. George · Satya P. Singh · Gary J. Myers · Gene E. Watson · Ingrid J. Pickering

Received: 11 December 2009 / Accepted: 12 February 2010

Abstract Human hair is frequently used as a bioindicator of mercury exposure. We have used X-ray absorption spectroscopy to examine the chemical forms of mercury in human hair samples taken from individuals with high fish consumption and concomitant exposure to methylmercury. The mercury is found to be predominantly methylmercury–cysteine or closely related species, comprising approximately 80% of the total mercury, with the remainder an inorganic thiolate-coordinated mercuric species. No appreciable role was found for selenium in coordinating mercury in hair.

Keywords Human hair · Mercury · X-ray absorption spectroscopy · Extended X-ray absorption fine structure · X-ray absorption near-edge spectra

Electronic supplementary material The online version of this article (doi:10.1007/s00775-010-0638-x) contains supplementary material, which is available to authorized users.

G. N. George (✉) · S. P. Singh · I. J. Pickering
Department of Geological Sciences,
University of Saskatchewan,
114 Science Place, Saskatoon,
SK S7N 5E2, Canada
e-mail: g.george@usask.ca

G. J. Myers
Department of Neurology and Pediatrics,
University of Rochester School of Medicine and Dentistry,
Rochester, NY 14642, USA

G. E. Watson
Eastman Institute for Oral Health,
University of Rochester School of Medicine and Dentistry,
Rochester, NY 14642, USA

Introduction

Fish is the major dietary source of potentially neurotoxic methylmercury species in human populations. Predatory marine fish such as swordfish and shark contain sufficiently high levels of methylmercury species that consumers are currently advised to eat these fish less frequently than once a month, and not at all if pregnant [1]. The precise nature of the methylmercury coordination in marine fish was only recently discovered to be an aliphatic thiolate, similar to the methylmercury–cysteine complex, using in situ X-ray absorption spectroscopy (XAS) [2]. More recently, it has been shown that this chemical form of mercury is not modified by digestion with simulated gastric fluid [3]. Mercury is excreted from the human body via a number of different routes. A fraction of the mercury in fish consumed as food probably cycles through the enterohepatic circulation, finally exiting in feces via sloughing of intestinal lumen cells, reducing the mercury dose absorbed into the body [4–6]. In agreement with this, Berntssen et al. [7] have reported that rats fed high-mercury fish show higher fecal excretion and lower tissue accumulation of mercury than rats consuming fish to which methylmercury chloride was added artificially. Although such mechanisms may eliminate some of the mercury ingested, there is continued concern that what remains could influence neurodevelopment. Another route of mercury excretion is via deposition of the metal into hair as it grows, and mercury may be excreted in mammals and birds by this route [8], although the fraction eliminated via this route has been estimated to be less than 10% [9].

Mercury levels in hair are a frequently used marker of mercury exposure in humans, and when the hair is long and analyzed segmentally, it can recapitulate a history of exposure [10]. The levels of mercury in newly formed hair

Published online: 12 March 2010

appear to be directly proportional to the concentrations found in blood and brain [11]. The hair to blood ratio in humans is approximately 250:1 [12, 13], although most animal studies indicate considerably lower ratios [12]. The high value appears to be specific to humans; in agreement with this, a ratio of 217:1 has recently been reported for human scalp hair transplanted into athymic nude mice [14]. It has been suggested that mercury enters hair and brain by similar mechanisms, and consequentially that hair can be considered to be a biological marker which is directly correlated with brain mercury exposure [11, 15].

Three large studies have been reported on the effects of dietary mercury on human populations. One study was located in the Faeroe Islands in the North Atlantic [16], the second in the Seychelles in the Indian Ocean [17], and the third in New Zealand [18]. The Faeroe Islands study was of a population with high dietary mercury primarily from pilot whale, but also from fish. The primary source of exposure in the New Zealand study was shark prepared as "fish and chips." The Seychelles study was of a population that consumes large quantities of fish that have mercury levels similar to those in oceanic fish consumed in North America. The studies reached different conclusions regarding the hazards of mercury exposure from fish consumption. Although the combined conclusions of these studies are still the subject of debate, all three used human hair as one indicator of mercury exposure, with blood and in the Faeroe Islands study chord blood as additional indicators. XAS is unique in that it is capable of determining the chemical form of any heavy element in situ, with no sample pretreatment required. In the work reported here, we used XAS to investigate the chemical nature of the mercury deposited in hair samples taken from three individuals with high dietary mercury owing to a high-fish diet in the Seychelles.

Materials and methods

X-ray absorption spectroscopy

XAS measurements were conducted at the Stanford Synchrotron Radiation Lightsource with the SPEAR storage ring containing between 90 and 100 mA at 3.0 GeV. Mercury L_{III}-edge and selenium K-edge data were collected on the structural molecular biology XAS beamline 9-3 operating with a wiggler field of 2 T and employing a Si(220) double-crystal monochromator. Beamline 9-3 is equipped with a rhodium-coated, vertically collimating mirror upstream of the monochromator, and a downstream bent-cylindrical focusing mirror (also rhodium-coated). Harmonic rejection was accomplished by setting the cutoff angle of the mirrors to reject energies above 15 keV. To minimize radiation damage, samples were maintained at a temperature of approximately 10 K in a liquid helium flow cryostat (Oxford Instruments, Abingdon, UK). X-ray absorption spectra were measured as the selenium $K\alpha_{1,2}$ or mercury $L\alpha_{1,2}$ fluorescence excitation spectra using a 30-element germanium array detector [19] with analog electronics (Canberra Corporation, Meriden, CT, USA) employing an amplifier shaping time of 0.125 μs. To avoid problems with nonlinearity of the detector due to high count-rates, X-ray filters (made of elemental As for Se, and Ga_2O_3 for Hg) were used to preferentially absorb scattered radiation. Silver Soller slits (EXAFS, Pioche, NV, USA) were optimally positioned between the sample and the detector to reduce filter fluorescence registered by the detector. Incident and transmitted XAS intensities were measured using nitrogen-filled ionization chambers. The mercury spectra were energy-calibrated with reference to the L_{III}-edge spectrum of Hg–Sn amalgam foil measured simultaneously with the data, the lowest energy inflection of which was assumed to be 12,285.0 eV. The selenium spectra were similarly energy calibrated with reference to the lowest-energy inflection of hexagonal elemental selenium, which was assumed to be at 12,658.0 eV. For near-edge spectra six sweeps were averaged, each of 25-min duration, whereas for the extended X-ray absorption fine structure (EXAFS) data set 36 individual sweeps were averaged, each of 35-min duration (totaling 21 h). Given the limited amount of synchrotron beam time available, the time required to collect individual data sets precluded the collection of data on large numbers of samples.

XAS data were processed using standard techniques and employing the EXAFSPAK program suite [20]. Near-edge spectra were fitted to linear combinations of standard spectra using the EXAFSPAK program DATFIT using the criteria previously described [3]. EXAFS oscillations were analyzed using ab initio theoretical phase and amplitude functions calculated using the program FEFF, version 7.02 [21, 22].

Sample preparation

Samples of scalp hair approximately 10 cm in length were obtained from individuals in the Seychelles, and were stored at room temperature prior to XAS. The hair was loosely packed into acrylic XAS sample cuvettes, which were frozen in liquid nitrogen immediately prior to insertion in the liquid helium cryostat for XAS measurements.

Results

X-ray absorption spectra arise from photoexcitation of a core electron, a $1s$ electron for a K edge, or a $2p_{3/2}$ electron

for an L_{III} edge. The spectrum can be arbitrarily divided into two overlapping regions—the near-edge spectrum, which is the structured region within approximately 50 eV of the absorption edge, and the EXAFS, which comprises oscillations on the high-energy side of the absorption edge and which can be accurately interpreted in terms of a local radial structure [23, 24]. The nomenclature of near-edge spectra is confusing [23] but this region is often referred to as the "X-ray absorption near-edge fine structure." The structure in near-edge spectra is due to transitions from the core level (1*s* for a K edge) to unoccupied molecular orbitals of the system. Intense transitions are Laporte-allowed $\Delta l = \pm 1$, and thus for K and L_{III} edges are to levels with a considerable *p* and *d* orbital character, respectively. Near-edge spectra are therefore sensitive to electronic structure, and give a fingerprint of the chemical species of the metal or metalloid concerned. The advantage of the near-edge region of the spectrum is that it can be quickly collected with good signal to noise. In contrast, EXAFS is more difficult to collect with adequate signal to noise, and its collection is not always practical for dilute samples. A unique benefit of XAS, both near-edge and EXAFS, is that it requires no pretreatment or extraction and thus provides a tool that can probe chemical species in situ.

Figure 1 shows the mercury L_{III} near-edge spectra of three hair samples from different individuals. The spectra of individual samples are very similar, with differences between them being smaller than the noise of the spectra (demonstrated by the difference spectra shown in Fig. 1). Principal component analysis [23] (not illustrated) confirmed that no additional components can be resolved from differences between the three spectra in Fig. 1. Because collection of EXAFS requires extensive signal averaging for dilute samples, a single representative hair sample was selected for study by EXAFS spectroscopy. Figure 2 shows the Hg L_{III} EXAFS and the results of a curve-fitting analysis, together with the EXAFS Fourier transforms. The signal-to-noise ratio of the data precluded analysis beyond $k = 11$ Å^{-1}, but nevertheless two distinct types of backscatterer are clearly observed as two peaks in the EXAFS Fourier transform (Fig. 2). Consistent with the two peaks observed in the Fourier transform, quantitative EXAFS curve-fitting analysis indicated the presence of two distinct backscatterers, one Hg–C at 2.06 Å and one Hg–S at 2.36 Å (Table 1). We note that minor components are very hard to detect in EXAFS data, especially if the data have low signal-to-noise content.

More information on the chemical composition can be obtained from analysis of the near-edge portion of the spectra [23]. Figure 3 shows the least-squares fit of the mercury L_{III} near-edge data of the sample of Fig. 2. The edge-fitting procedure was applied for two- and three-component fits, but in the latter the third component was found to be not statistically significant in any of the cases tested, being rejected by the algorithm [23]. A major component of methylmercury–cysteine was consistently

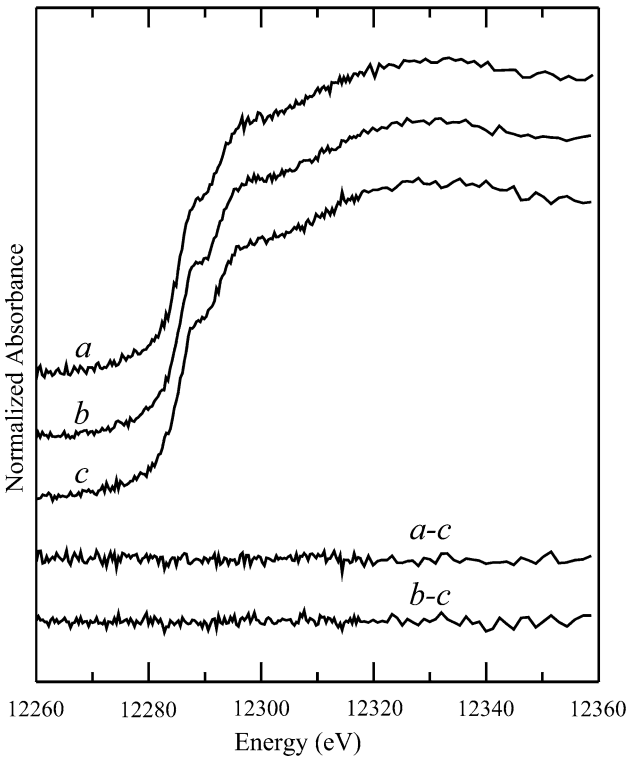

Fig. 1 Comparison of mercury L_{III} near-edge spectra of hair samples from three individuals. The differences between adjacent spectra are shown beneath, illustrating that the three samples have chemical compositions that are indistinguishable by analysis of near-edge spectra

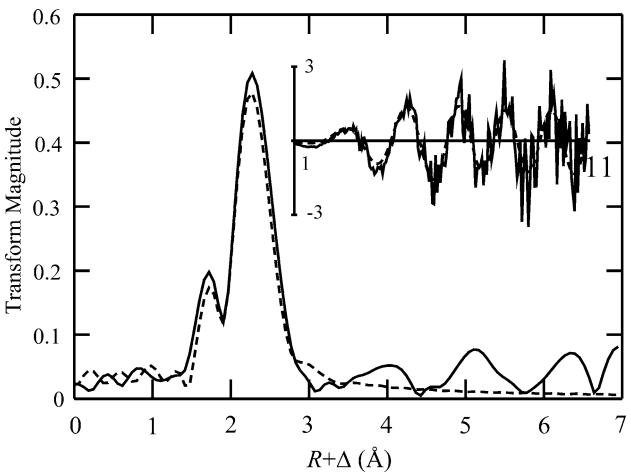

Fig. 2 Hg L_{III} extended X-ray absorption fine structure (EXAFS) Fourier transforms of hair sample a (Fig. 1) with Hg–S phase correction. The *inset* shows the raw k^3-weighted EXAFS data. The *solid line* shows the experimental data, and the *dashed line* shows the best fit

Table 1 Structural parameters for mercury in hair compared with those of L-cysteinato(methyl)mercury(II) in both the crystalline and the solution state

Hg–C			Hg–S			ΔE_0 (eV)	F
N[a]	R (Å)	σ^2 (Å^2)	N[a]	R (Å)	σ^2 (Å^2)		
Hair EXAFS							
1	2.06 (1)	0.003 (2)	1	2.356 (4)	0.0023 (5)	−16.5[b]	0.65
0.77[c]	2.03 (1)	0.003 (2)	1.46	2.357 (4)	0.0051 (5)	−16.5[b]	0.64
0.77[d]	2.05 (1)	0.002 (2)	0.77	2.33 (1)	0.002 (1)	−16.5[b]	0.64
			0.69	2.42 (1)	0.004 (2)		
L-Cys-$HgCH_3$ crystallography [27]							
1	2.098	–	1	2.352	–	–	
L-Cys-$HgCH_3$ EXAFS [28]							
1	2.070 (3)	0.0020 (2)	1	2.351 (2)	0.0029 (1)	−16.5 (5)	0.29

The values in *parentheses* are the estimated standard deviations obtained from the diagonal elements of the covariance matrix. The fit-error function F is defined by $F = \sqrt{\sum k^6(\chi(k)_{\text{calcd}} - \chi(k)_{\text{expt}})^2 / \sum \chi(k)^2_{\text{expt}}}$, where $\chi(k)$ are the extended X-ray absorption fine structure (*EXAFS*) oscillations and k is the photoelectron wave number given by $k = \sqrt{\frac{2m_e}{\hbar^2}(E - E_0)}$

N coordination numbers, R interatomic distances, σ^2 Debye–Waller factors (the mean-square deviations in interatomic distance), ΔE_0 the threshold energy shifts

[a] The values for the coordination numbers were not refined owing to high mutual correlation with the Debye–Waller factors

[b] Because of the limited k-range, the ΔE_0 value was constrained to the value obtained from fitting the EXAFS data of a large number of methylmercury model compounds with k range 16 Å^{-1} and above (not illustrated)

[c] Alternative fit based on the results of the near-edge analysis, with 77% of a two-coordinate CH_3HgS species, and 23% of a three-coordinate $[Hg(SR)_3]^-$ species, assuming unresolved Hg–S bond lengths

[d] Alternative fit based on the results of the near-edge analysis, with 77% of a two-coordinate CH_3HgS species, and 23% of a three-coordinate $[Hg(SR)_3]^-$ species, with the refinement starting from the typical Hg–S bond lengths for two- and three-coordinate species

required for an adequate fit, and essentially equivalent best fits were obtained for different minor components corresponding to mercury coordinated to aliphatic thiolates. For this minor component, compounds with three and with four thiolate donors ($[Hg(SR)_3]^-$ and $[Hg(SR)_4]^{2-}$, respectively) gave essentially equivalent fits. As expected, linear combination fitting of the data from all three hair samples gave essentially indistinguishable fits. These results are summarized in Table 2. The near-edge analyses are in excellent agreement with the results of conventional analysis of Seychellois hair [11], which indicated that approximately 80% of the mercury is present as methylmercury forms and approximately 20% as inorganic forms.

The presence of 23% $[Hg(SR)_3]^-$ in the hair might be expected to affect the EXAFS data. An alternative fit is presented in Table 1, with 77% of interactions expected for methylmercury bound to sulfur (0.77 Hg–C and 0.77 Hg–S) plus 23% of the longer Hg–S interaction corresponding to the inorganic species determined by fitting the near-edge spectra (0.23 × 3 Hg–S). As discussed above, Hg–S bond lengths of 2.34 and 2.44 Å are expected for two- and three-coordinate mercury, respectively. The EXAFS-resolution ΔR can be defined as the smallest difference in interatomic distance that can be discriminated

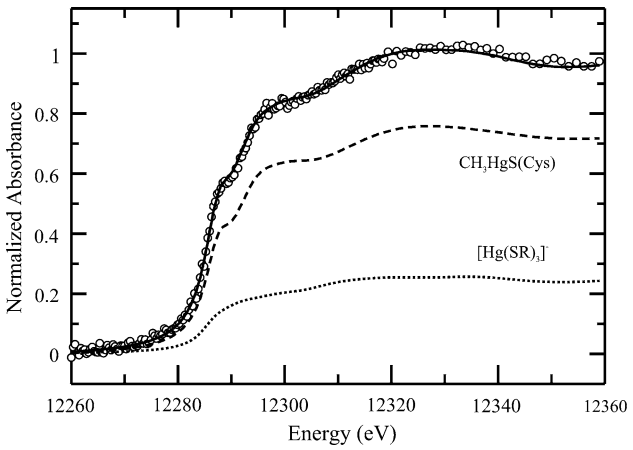

Fig. 3 Linear combination analysis of mercury L_{III} X-ray absorption near-edge spectra of hair. The *circles* show the experimental hair spectrum, the *solid line* shows the best fit, and the *dashed line* and the *dotted line* show the spectra of individual components, methylmercury–cysteine (*dashed line*) 77 ± 3% and $[Hg(S^tBu)_3]^-$ (*dotted line*) 23 ± 3% (errors are estimated standard deviations obtained from the diagonal elements of the covariance matrix)

for similar backscatterers, and to a first approximation this is given by $\Delta R \approx \pi/2\ k$, where k is the extent of the data in units of per angstrom. We note that our EXAFS data lack

Table 2 Linear combination analysis of mercury L_{III} near-edge spectra of human hair

Sample	$CH_3Hg(Cys)$ (%)	$[Hg(SR)_3]^-$ (%)	f ($\times 10^4$)[a]
a	77 (3)	23 (3)	1.35
b	80 (3)	20 (3)	1.37
c	81 (3)	19 (3)	1.36

[a] The fit error f is defined as $f = \frac{1}{n}\sum (A_{obsd} - A_{calc})^2$, where A is the normalized X-ray absorbance and n is the number of data points within range. We estimate from Fourier filtering that the contribution to f from high-frequency noise is close to 0.8×10^{-4} in all three cases. When only a single component was used to fit the data, then $CH_3Hg(Cys)$ provided the best fits, with f increased by 0.47×10^{-4}, 0.46×10^{-4}, and 0.49×10^{-4} for samples a, b, and c, respectively (one- and two-component fit residuals are shown in Fig. S1)

the k range to properly resolve the bond lengths of two- and three-coordinate components, but nevertheless the fit shown in Table 1 indicates that the EXAFS data are consistent with the near-edge analysis, with somewhat smaller Debye–Waller factors for the short Hg–S components, and larger estimated standard deviations for all parameters. Alternatively, the use of higher effective Hg–S coordination numbers, and slightly lower effective Hg–C coordination numbers (Table 1) derived from the near-edge analysis also gives a very slight improvement in the fit. The improvement in the fit errors for both alternative fits is marginal and although we can conclude that the EXAFS data are fully consistent with the near-edge analysis, our data are not of sufficient quality to answer detailed questions on coordination numbers. Nevertheless, the observation of significant Hg–C EXAFS clearly indicates that the majority of the mercury present is methylmercury, with sulfur donors completing the metal coordination environment.

Discussion

The XAS data presented herein provide clear evidence concerning the chemical speciation of mercury in human hair. Our data are in agreement with and extend the results from conventional chemical analysis, which showed Seychellois hair to contain approximately 80% of the total mercury as methylmercury forms, with the remainder in inorganic forms [11]. Different proportions of methylmercury and inorganic forms are found in other populations [25, 26]. The EXAFS-derived bond lengths are in excellent agreement with those reported for the methylmercury complex with cysteine. The values from X-ray crystallography for Hg–C and Hg–S are 2.098 and 2.352 Å [27], respectively, and from EXAFS spectroscopy of solutions of methylmercury–cysteine they are 2.07 and 2.35 Å [28] (Table 1). Stable complexes are known with two $[Hg(SR)_2]$, three $[Hg(SR)_3]^-$, or four $[Hg(SR)_4]^{2-}$ coordination, and well-characterized examples of all three coordination modes have been identified by X-ray crystallography [29]. A four-coordinate cysteine complex $[Hg(Cys)_4]$ has recently been reported to be formed in aqueous solutions at high pH values [30]. The Hg–S bond length is highly characteristic of the coordination [31]. The Cambridge Crystal Structure Database [32] indicates typical Hg–S bond lengths of 2.34, 2.44, and 2.55 Å for two-, three-, and four-coordinate compounds, respectively. No coordination compounds containing sulfur coordinated by four mercury atoms are listed in the Cambridge Crystal Structure Database [32], although this structure is found in black mercuric sulfide, otherwise known as β-HgS or metacinnabar, which has the zinc blende structure with tetrahedral coordination of mercury by sulfur, and tetrahedral coordination of sulfur by mercury, with an Hg–S bond length of 2.55 Å [33].

Li et al. [26] recently reported an XAS study of human hair from individuals exposed in a heavily contaminated elemental mercury mine site area. Conventional analysis showed predominantly inorganic mercury [26], contrasting with methylmercury exposure from fish consumption. Li et al. [26] reported both sulfur K and mercury L_{III} near-edge and EXAFS data of human hair. From the mercury EXAFS, Li et al. determined three Hg–S interactions with a 2.48-Å bond length, consistent with mercury coordinated by three sulfurs. However, Li et al.'s [26] analysis of the sulfur EXAFS yielded four S–Hg interactions at 2.36 Å, a bond length neither consistent with that from mercury EXAFS nor characteristic of four-coordinate sulfur. Furthermore, the 0.0084 wt% mercury content [26] contrasts with about 18 wt% sulfur in normal human hair [34], and corresponds to less than one mercury atom per 10,000 sulfur atoms. We conclude that sulfur K-edge measurements of hair cannot possibly detect mercury backscatterers. The sulfur near-edge spectra [26] strongly resemble those of cystine disulfide species [35], the form expected in extracellular environments such as hair [35]; the sulfur EXAFS are likely due to unresolved S–C and S–S from disulfide species. Four mercury backscatterers have a much larger amplitude than do a single sulfur or carbon, and distinguishing these backscatterers would normally be relatively simple. However, several factors can complicate assignment, such as if the threshold energy shift ΔE_0 is allowed to refine outside reasonable bounds [36], although ΔE_0 values were not listed by Li et al. [26]. Very large, physically unrealistic Debye–Waller factors, such as 0.025 $Å^2$ [26], severely reduce EXAFS amplitudes except at lower k values. Fourier filtering with window functions, which have to be used, severely reduce amplitudes at low k. These factors may have led Li et al. to form erroneous conclusions from the sulfur EXAFS.

We now return to the major question addressed here, the chemical nature of mercury in human hair. From a simple chemical point of view, the high sulfur content of hair (discussed above) might argue for sulfur donors to mercury. However, as we have discussed above, the sulfur is essentially present as oxidized disulfide cystine, and thus could not directly provide thiolate donors to mercury. The molecular toxicological effect of mercury is often associated with selenium [37, 38], and because the mercury L_{III} near-edge spectra from compounds containing Hg–S and Hg–Se coordination can sometimes be difficult to distinguish [3], we also examined the selenium K-edge spectra of hair. The relative levels of mercury and selenium can be estimated from a combination of the selenium K and mercury L_{III}-edge jumps and the selenium $K\alpha_{12}$ and mercury $L\alpha_{12}$ fluorescence intensities, correcting for fluorescence yields [39], and this indicates that the selenium levels are approximately 43% of the mercury levels. Figure 4 shows the near-edge spectrum of the hair sample of Figs. 2 and 3, together with the analysis of the near-edge spectrum. The spectrum could be adequately analyzed without any model spectra typifying Hg–Se coordination [3] and instead could be adequately modeled using oxidized selenium species such as selenocystine [40] with a small amount of selenite (Fig. 4). This together with the mercury L_{III} near-edge and EXAFS analysis indicates that selenium plays no significant role in coordination of mercury in human hair.

Although fish are the major source of mercury exposure in the Seychelles, dental amalgam is an alternative potential source of the mercury in hair. The amalgam status of the individuals from which hair was sampled is unknown, but this is unlikely to be a major factor because it is well established that there is no correlation between hair mercury levels and numbers of dental amalgams [41]. Any large-scale influence of amalgam on our results is therefore unlikely, but mobilization of mercury from dental amalgam and subsequent methylation by microflora (oral and gut) cannot rigorously be excluded as an additional potential source of some of the methylmercury found in hair.

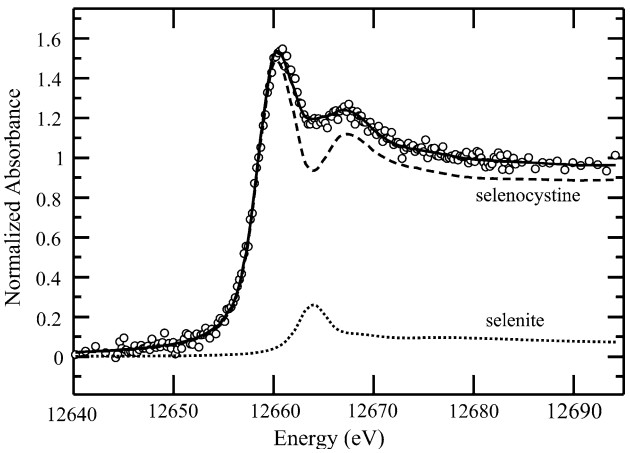

Fig. 4 Linear combination analysis of selenium K X-ray absorption near-edge spectra of hair. The *circles* show the experimental hair spectrum, the *solid line* shows the best fit, and the *dashed line* and the *dotted line* show the spectra of individual components, selenocystine (*dashed line*) 91 ± 4% and selenite (*dotted line*) 9 ± 3% (errors are estimated standard deviations obtained from the diagonal elements of the covariance matrix)

Previous work indicates that methylmercury–cysteine is actively transported as a substrate for human L-type large neutral amino acid transporter (LAT), and that this is responsible for its uptake into cells [5]. We have shown that this cannot be due to a methionine-specific molecular mimicry as previously assumed, but is rather due to a nonspecific neutral amino acid activity [28]. Assuming that this is correct, our results show that no major changes in mercury coordination occur on accumulation into hair. As discussed above, remarkable levels of mercury concentration occur in human hair, at around 250 times blood levels [12, 13]. A similarly remarkable concentration of methylmercury–cysteine has recently been observed in zebrafish larvae in the rapidly proliferating single layer of cells comprising the lens epithelia [42]. Recent work using autoradiography of human scalp hair transplanted into athymic nude mice has shown that most of the mercury taken up is concentrated in the hair shafts and in the keratogenous zone of the hair follicle [14]. Both hair keratinocytes and lens epithelial cells are engaged in significant protein synthesis. Given that LAT expression is known to be related to protein synthesis, the explanation for both of these accumulations may be as simple as increased methylmercury–cysteine transport due to increased transporter levels. Furthermore, it has been shown that the LAT 1 isoform of the transporter is selectively expressed at the blood–brain barrier [43], suggesting a role for the transporter in brain accumulation of methylmercury–cysteine. Transport of inorganic mercury species and that of methylmercury species are likely to be different. Recent work on sea urchin embryos indicates that inorganic mercury species are exported by MRP/ABCC-type transporters, whereas methylmercury species are not [44]. The presence of inorganic mercury species in hair could potentially arise from two sources, either a mechanism exists for directly incorporating inorganic mercury into hair or a fraction of the methylmercury in hair is demethylated subsequent to incorporation. The latter could arise via coordination of mercury by more than one thiolate, which would increase the negative charge on the methyl group [45] and promoting C–Hg protonolysis to yield methane and inorganic mercury. Further work is required to determine which of these two mechanisms is in effect.

Concluding remarks

We have shown that the predominant chemical form of mercury in human hair strongly resembles methylmercury–cysteine with Hg–C and Hg–S bond lengths of 2.06 and 2.36 Å, respectively. The analysis of the near-edge spectra agrees with that of the EXAFS analysis, and also indicates approximately 20% of inorganic mercury is a high-nuclearity aliphatic thiolate complex, probably either $[Hg(SR)_3]^-$ or $[Hg(SR)_4]^{2-}$. No involvement of selenium in coordination of mercury is indicated from analysis of mercury L_{III}-edge and selenium K-edge X-ray absorption spectra. Because the mechanisms of uptake in brain and hair are thought to be related, our finding that methylmercury–cysteine is incorporated into hair may be relevant to the mechanism of neurotoxicity of methylmercury species.

Acknowledgments This work was supported by the Canadian Institutes for Health Research, by Canada Research Chair awards (G.N.G. and I.J.P.), by the Natural Sciences and Engineering Research Council (Canada), and by the National Institute of Environmental Health Sciences (Environmental Health Sciences Center Grant P30-ES01247). Portions of this work were also carried out at the Stanford Synchrotron Radiation Lightsource, which is funded by the US Department of Energy, Office of Basic Energy Sciences. The Structural Molecular Biology program is funded by the US Department of Energy, Office of Biological and Environmental Sciences and by the National Institutes of Health, National Center for Research Resources, Biomedical Technology Program. We thank members of the George/Pickering research group for contributions to data collection.

References

1. US Food and Drug Administration (2004) What you need to know about mercury in fish and shellfish. http://www.cfsan.fda.gov/~dms/admehg3.html
2. Harris HH, Pickering IJ, George GN (2003) Science 301:1203
3. George GN, Singh SP, Prince RC, Pickering IJ (2008) Chem Res Toxicol 21:2106–2110
4. Norseth T, Clarkson TW (1971) Arch Environ Health 22:568–577
5. Simmons-Willis TA, Koh AS, Clarkson TW, Ballatori N (2002) Biochem J 367:239–246
6. Wortelboer HM, Balvers MGJ, Usta M, van Bladeren PJ, Cnubben NHP (2008) Environ Toxicol Pharmacol 28:102–108
7. Berntssen MHG, Hylland K, Lundebye A-K, Julshamn K (2004) Food Chem Toxicol 42:1359–1366
8. Thompson DR (1996) In: Beyer WN, Heinz GH, Redmon-Norwood AW (eds) Environmental contaminants in wildlife: interpreting tissue concentrations. CRC Press, Boca Raton, pp 341–356
9. Magos L, Clarkson TW (2008) Toxicol Lett 182:48–49
10. Cox C, Clarkson TW, Marsh DO, Amin-Zaki L, Tikriti S, Myers G (1989) Environ Res 49:318–332
11. Cernichiari D, Brewer R, Myers GJ, Marsh DO, Lapham LW, Cox C, Shamlaye CF, Berlin M, Davidson PW, Clarkson TW (1995) Neurotoxicology 16:705–710
12. WHO (1990) Environmental health criteria 101, methyl mercury. World Health Organization, Geneva
13. Clarkson TW (1997) Crit Rev Clin Lab Sci 34:369–403
14. Zareba G, Cernichiari E, Goldsmith LA, Clarkson TW (2008) J Appl Toxicol 28:535–542
15. Cernichiari E, Myers GJ, Ballatoria N, Zarebaa G, Vyasc J, Clarkson T (2007) Neurotoxicology 28:1015–1022
16. Choi AL, Grandjean P (2008) Environ Chem 5:112–120
17. Myers GJ, Thurston SW, Pearson AT, Davidson PW, Cox C, Shamlaye CF, Cernichiari E, Clarkson TW (2009) Neurotoxicology 30:338–349
18. Goyer RA, Aposhian HV, Arab L, Bellinger DC, Burbacher TM, Burke TA, Jacobson JL, Knobeloch LM, Ryan LM, Stern AH, Committee on the Toxicological Effects of Methylmercury (2000) National Research Council, toxicological effects of methylmercury. National Academy Press, Washington
19. Cramer SP, Tench O, Yocum M, George GN (1998) Nucl Instrum Methods A 266:586–591
20. George GN (2000) EXAFSPAK. http://ssrl.slac.stanford.edu/exafspak.html
21. Rehr JJ, Mustre de Leon J, Zabinsky SI, Albers RC (1991) J Am Chem Soc 113:5135–5140
22. Mustre de Leon J, Rehr JJ, Zabinsky SI, Albers RC (1991) Phys Rev 44:4146–4156
23. George GN, Pickering IJ (2007) In: Tsakanov V, Wiedemann H (eds) Brilliant light in life and materials sciences. Springer, Dordrecht, pp 97–119
24. George GN, Pickering IJ, Doonan CJ, Korbas M, Singh SP, Hoffmeyer R (2008) Adv Mol Toxicol 2:125–155
25. Marika Berglund M, Lind B, Björnberg KA, Palm B, Einarsson O, Vahter M (2005) Environ Health 4:20
26. Li Y-F, Chen C, Li B, Li W, Qu L, Dong Z, Nomura M, Gao Y, Zhao J, Hu W, Zhao Y, Chai Z (2008) J Inorg Biochem 102:500–506
27. Taylor NJ, Wong YS, Chieh PC, Carty AJ (1975) J Chem Soc Dalton Trans 5:438–442
28. Hoffmeyer R, Singh SP, Doonan CJ, Ross ARS, Hughes RJ, Pickering IJ, George GN (2006) Chem Res Toxicol 19:753–759
29. Govindaswamy N, Moy J, Millar M, Koch SA (1992) Inorg Chem 31:5343–5344
30. Jalilehvand F, Leung BO, Izadifard M, Damian E (2006) Inorg Chem 45:66–73
31. George GN, Prince RC, Gailer J, Buttigieg GA, Denton MB, Harris HH, Pickering IJ (2004) Chem Res Toxicol 17:999–1006
32. Allen FH, Kennard O, Watson DG (1994) Struct Correl 1:71–110
33. Makeev AA, Kopatskii NA (1969) Sov Phys J 12:160
34. Wilson RH, Lewis HB (1927) J Biol Chem 73:543–553
35. Pickering IJ, Prince RC, Divers TC, George GN (1998) FEBS Lett 441:11–14
36. Clark-Baldwin K, Tierney DL, Govindaswamy N, Gruff ES, Kim C, Berg J, Koch SA, Penner-Hahn JE (1998) J Am Chem Soc 120:8401–8409
37. Gailer J, George GN, Pickering IJ, Madden S, Prince RC, Yu E, Denton MB, Younis HS, Aposhian HV (2000) Chem Res Toxicol 13:1135–1142
38. Gailer J (2007) Coord Chem Rev 251:234–254
39. Krause MO (1979) J Chem Phys Ref Data 8:307–327
40. Pickering IJ, George GN, van Fleet-Stalder V, Chasteen TC, Prince RC (1999) J Biol Inorg Chem 4:791–794
41. Clarkson TW, Magos L (2007) Crit Rev Toxicol 36:609–662
42. Korbas M, Blechinger S, Krone PH, Pickering IJ, George GN (2008) Proc Natl Acad Sci USA 105:12108–12112
43. Boado RJ, Li JY, Nagaya M, Zhang C, Pardridge WM (1999) Proc Natl Acad Sci USA 96:12079–12084
44. Bošnjak I, Uhlinger KR, Heim W, Smital T, Franekić-Čolić J, Coale K, Epel D, Hamdoun A (2009) Environ Sci Technol 43:8374–8380
45. Ni B, Kramer JR, Bell RA, Werstiuk NH (2006) J Phys Chem A 110:9451–9458